Journal of Applied Polymer Science

Nanostructures and Surface Nanomechanical Properties of Polyacrylonitrile/Graphene Oxide Composite Nanofibers by Electrospinning

Qingqing Wang,[1] Yuanzhi Du,[1] Quan Feng,[2] Fenglin Huang,[1] Keyu Lu,[3] Jingyan Liu,[1] Qufu Wei[1]

[1]Key Laboratory of Eco-Textiles, Jiangnan University, Wuxi 214122, China

[2]Textiles and Clothing Department, Anhui Polytechnic University, Wuhu 241000, China

[3]State Key Laboratory of Food Science and Technology, Wuxi 214122, China

Correspondence to: Q. Wei (E-mail: qfwei@jiangnan.edu.cn)

ABSTRACT: In this work, polyacrylonitrile (PAN)/graphene oxide (GO) composite nanofibers were prepared by a facile compounding and electrospinning processes. A small amount of GO powders were first dispersed in *N*,*N*-dimethylformamide by sonication, and then, PAN powders were added to prepare an electrospinning solution. The surface morphology was analyzed by atomic force microscopy and transmission electron microscopy, whereas the chemical properties of the PAN and PAN/GO composite nanofibers were compared by infrared (IR) spectroscopy. Also, lateral force microscopy and force–distance curves (FDC) were employed to investigate the surface properties, such as friction force and elasticity. The experimental results indicate that with increasing GO concentration, the surface friction force and adhesive force increased, so the nanofibers showed promise for applications as supports for enzyme immobilization. © 2012 Wiley Periodicals, Inc. J. Appl. Polym. Sci. 000: 000–000, 2012

KEYWORDS: composites; electrospinning; fibers; mechanical properties; morphology

Received 5 May 2012; accepted 29 June 2012; published online
DOI: 10.1002/app.38273

INTRODUCTION

Polyacrylonitrile (PAN) is a commercially important polymer because it is the precursor for about 90% of carbon fibers manufactured today.[1] Recently, carbon nanofibers have been widely investigated as high-performance materials because of their superior properties and extensive applications,[2] so electrospun PAN nanofiber precursors with diameters ranging from 100 nm to 1.2 μm have been reported.[3] Apart from carbon precursors, PAN nanofibers themselves have attracted a great deal of attention because of a variety of their excellent characteristics, including thermal stability, resistance to most solvents, high strength, and so on. Some nanofillers, including single-walled or multiwalled carbon nantubes[4] and montmorrilonite,[2] have been added to the polymer matrix to prepare composite PAN nanofibers with improved mechanical strength, electrical conductivity, mechanical strength, and thermal stability. However, the relative poor hydrophilicity and biocompatibility prevent PAN nanofibers from potential applications in biomaterials.

Graphene oxide (GO), containing a range of oxygen functional groups,[5] is an ideal candidate for use in various applications, especially in bioelectrochemistry. Nonfully oxidized GO maintains an sp^2 hybridized network. Such GO supports the efficient electrical wiring of the redox centers of several heme-containing metalloproteins to the electrode. Significantly, proteins retain their structural integrity and biological activity upon forming mixtures with GO.[6] Recently, there has been increasing interest in polymer–GO composites because of their outstanding physical, chemical, and mechanical properties[7] and their improved biocompatibility.

PAN/GO composite nanofibers can be good candidates for enzyme immobilization and may have great potential in bioelectrochemistry. As a support for enzyme immobilization, the surface properties like microstructure, elasticity and surface friction force are very important factors. However, there has been no literature on detailed surface characterization of these composite nanofibers. In this work, atomic force microscopy (AFM), lateral force microscopy (LFM), and force–distance curves were employed to investigate the surface properties of PAN/GO composite nanofibers.

EXPERIMENTAL

Materials

GO was purchased from XF Nano, Inc. The PAN (weight-average molecular weight = 79,100) powder was obtained from

Applied Polymer SCIENCE

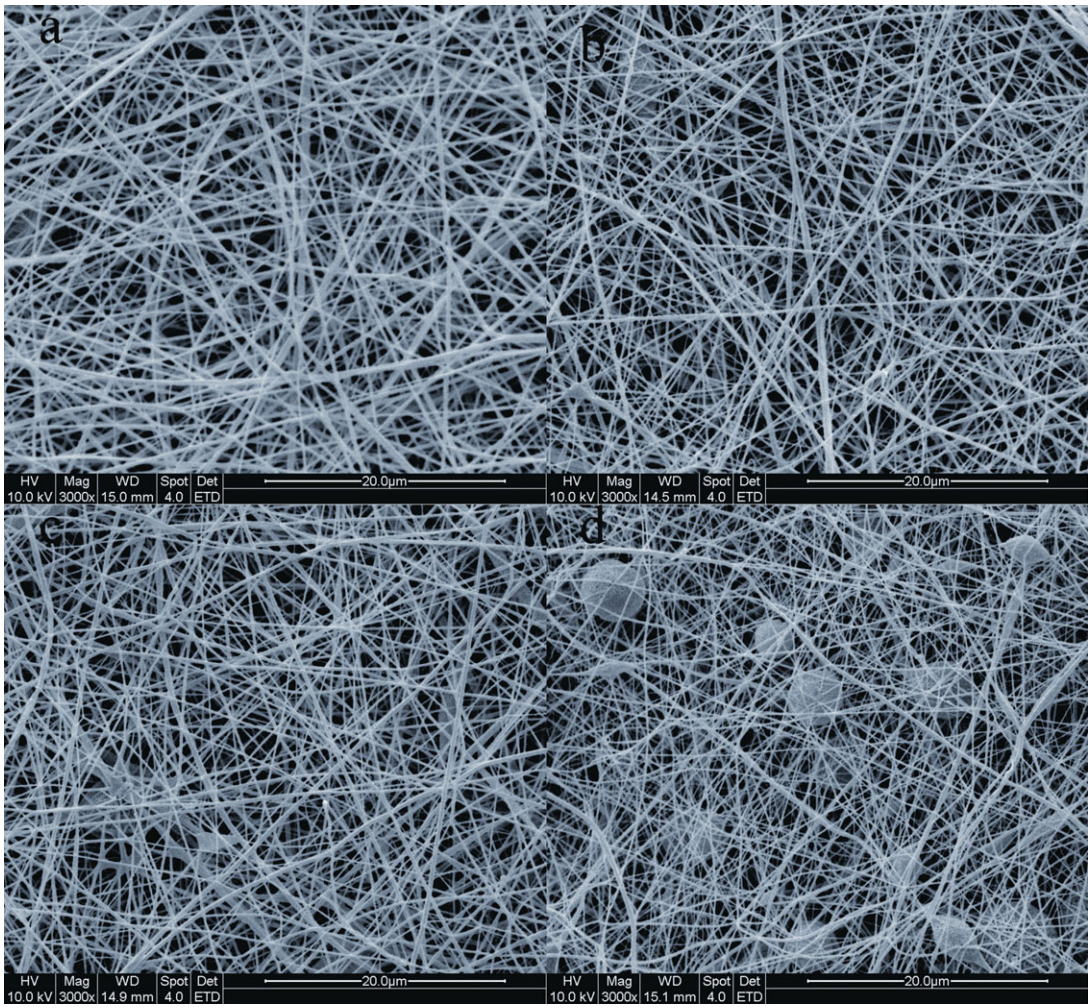

Figure 1. (a–d) SEM and (e,f) TEM images of PAN and PAN/GO composite nanofibers: (a) PAN, (b) PAN/GO-0.05, (c) PAN/GO-0.1, and (d) PAN/GO-0.5. [Color figure can be viewed in the online issue, which is available at wileyonlinelibrary.com.]

Aldrich and used without further purification. 99.5% *N,N*-dimethylformamide (DMF) was used as received.

Fabrication of the Composite Nanofibers

A certain amount of GO was added to 20 mL of DMF and fully dissolved by sonication for 2 h. Then PAN (10 wt %) powders were dispersed in the GO/DMF slurry by magnetic stirring for 8 h to prepare electrospinning solution. The composite electrospinning solution was electrospun at a positive voltage of 15 kV with a working distance of 15 cm, and the flow rate was set as 1.5 mL/h. The mass ratio of the GO to PAN was 0.05 wt %, 0.1 wt %, and 0.5 wt % and is referred to as PAN/GO-0.05, PAN/GO-0.1, and PAN/GO-0.5, respectively.

Characterization

AFM and LFM (Benyuan CSPM 4000, China) were used in this work to analyze the surface morphology and surface nanotribology as well as the nanomechanical properties of the PAN/GO composite nanofibers. The AFM images were obtained in tapping mode, whereas the LFM and FDC were acquired in contact mode. All images and curves were obtained at ambient conditions. Besides, high-resolution transmission electron microscopy (HRTEM; JEOL-2100, Japan) was also employed here to investigate the internal structure of the composite nanofibers.

The chemical properties of the electrospun nanofibers with and without GO were investigated and compared by Fourier Transform Infrared Spectroscopy (FTIR, Nicolet Nexus, Thermo Electron Corp.) in the range 4000–650 cm^{-1}, using attenuated total reflection method. The spectra were recorded with 32 scans with a resolution of 4 cm^{-1}.

RESULTS AND DISCUSSION

Effects of GO Addition on the Structure of the Composite Nanofibers

Figure 1(a–d) shows the SEM images of electrospun PAN/GO composite nanofibers from 10 wt % PAN solutions with different GO concentrations (0, 0.05, 0.1, and 0.5 wt %) under the same conditions. The nanofibers were randomly distributed to form the fibrous web. It can be observed that the electrospun nanofibers had variable fiber diameters and structure, which was significantly affected by the addition of GO. With the increase of GO loading, the average diameters of the composite nanofibers were decreased. Besides, the composite electrospun

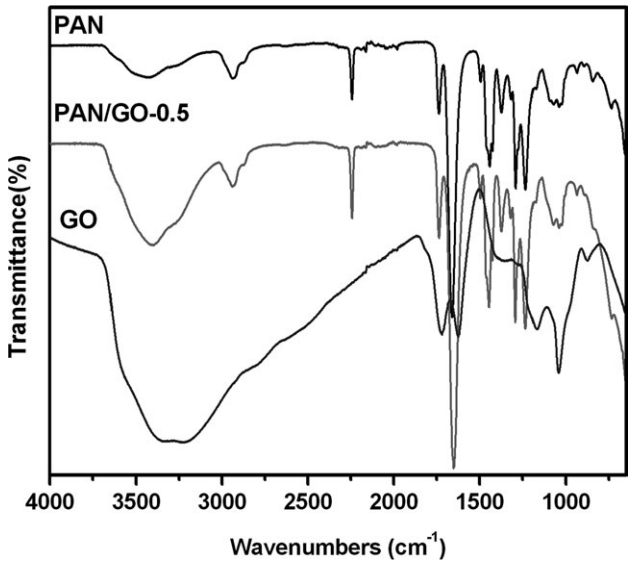

Figure 2. FTIR spectra of the PAN, GO, and PAN/GO nanofibrous membranes.

PAN nanofibers with GO as nanofillers were uniform in diameter, but some beaded structures of the nanofibers were formed. It is well known that parameters of the polymer solution, such as molecular weight, solution viscosity, surface tension, solution conductivity and dielectric constant are critical factors that affect the morphology of electrospun fiber.[8–10] A small amount of GO can remarkably change the solution properties of PAN.[11] Because GO can be poorly dispersed in DMF,[12] the composite polymer solution can be divided into GO-rich domain and GO-scarce domain, which may lead to instability of the liquid jet during electrospinning process. So, the beaded structures were formed.

FTIR Analysis

The FTIR spectra of PAN, GO and PAN/GO nanofibers are presented in Figure 2. The band at 2240 cm^{-1} can be assigned to nitrile groups, whereas those at 2930 and 1454 cm^{-1} can be ascribed to C—H stretching vibration of —CH_2. The peak observed at 1740 cm^{-1} can be attributed to C=O stretching vibration, of which carbonyl bands came from methyl acrylate comonomer.[13] The GO spectrum reveals the C—O—C stretching vibration band at 1250 cm^{-1}, the C—O band at 1053 cm^{-1}, as well as C=O in carboxylic acid and carbonyl moieties at 1715 cm^{-1}.[14] The resonance at 1621 cm^{-1} could be due to the vibrations of the adsorbed water molecules or the skeletal vibrations of nonoxidized graphitic domains.[15] The broad band at 3430 cm^{-1} indicates that the nanofibers contain O—H group on their surface due to adsorbed water.[16] The PAN and PAN/GO curves are quite similar and no new characteristic peaks can be observed, indicating that the chemical structure of PAN was not changed and no chemical bond was formed between PAN chains and GO.

Effect of GO Addition on the Topography and Lateral Force

The principle of AFM and LFM was displayed in Figure 3. During a typical process, the sample is placed on the scanner, of which the piezoceramic tube can move independently in x, y and z directions under impressed voltage. The laser irradiates on the back of the tip and after reflection, it is situated on the position detector. The difference of light intensity at the vertical direction leads to voltage difference. The variation of spot position can be obtained by measuring the voltage difference.

In the contact mode, the tip of the probe partially keeps contacting with the surface of the sample. During the process of scanning the sample surface, due to the interaction force between the atoms of the sample surface and the atoms of probe tip, the cantilever will move up and down according to the surface morphology of the sample, the reflected light will displace correspondingly, and thus the value of voltage difference is also changed. The feedback circuit measures this value and keeps it fixed by changing the voltage loaded on the vertical direction. This voltage is recorded and gives information of the topography.

Although the topographic information is obtained from the vertical displacements of the tip (typically, the displacement of the z-axis piezo), the friction properties can be recorded by the lateral torsion of the cantilever during scanning the sample in both directions.

The surface morphology of the electrospun PAN and PAN/GO nanofibers was investigated using AFM [Figure 4(a–d)]. The individual nanofibers with variable diameters were randomly distributed on the mica plate. The surface of the pure PAN nanofibers [Figure 4(a)] was relatively smooth, with a clear fibril structure and a wrinkle-like morphology. At the point that two individual nanofibers contact, the upper nanofiber was bent but not collapsed, which means the pure PAN nanofiber, was comparatively rigid. With the increase of GO content, the surface became coarser and more irregular. Grooves could be seen on the surface of the composite nanofibers with 0.05 wt % GO, as presented in Figure 4(b). When the GO content reached 0.1 wt % and 0.5 wt % [Figure 4(c,d)], the nanofibers became adhesive and the nanofiber would collapse at the meeting point of two nanofibers, which means that the elasticity of the nanofibers increased with the addition of GO.

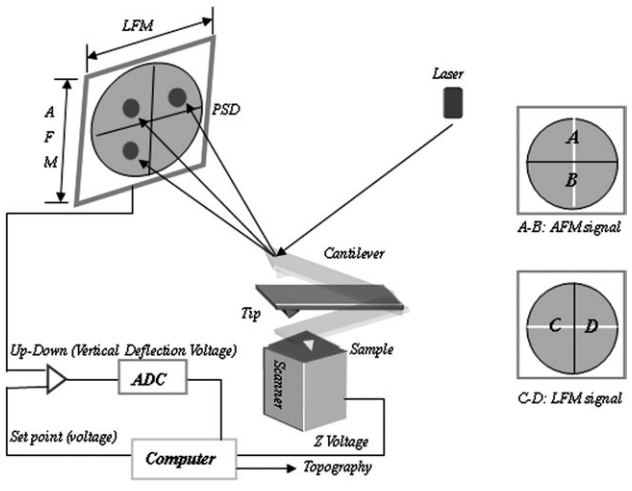

Figure 3. Schematic illustration of the principle of AFM and LFM. (PSD:Phase-Sensitive Detector; ADC: Analog To Digital Converter).

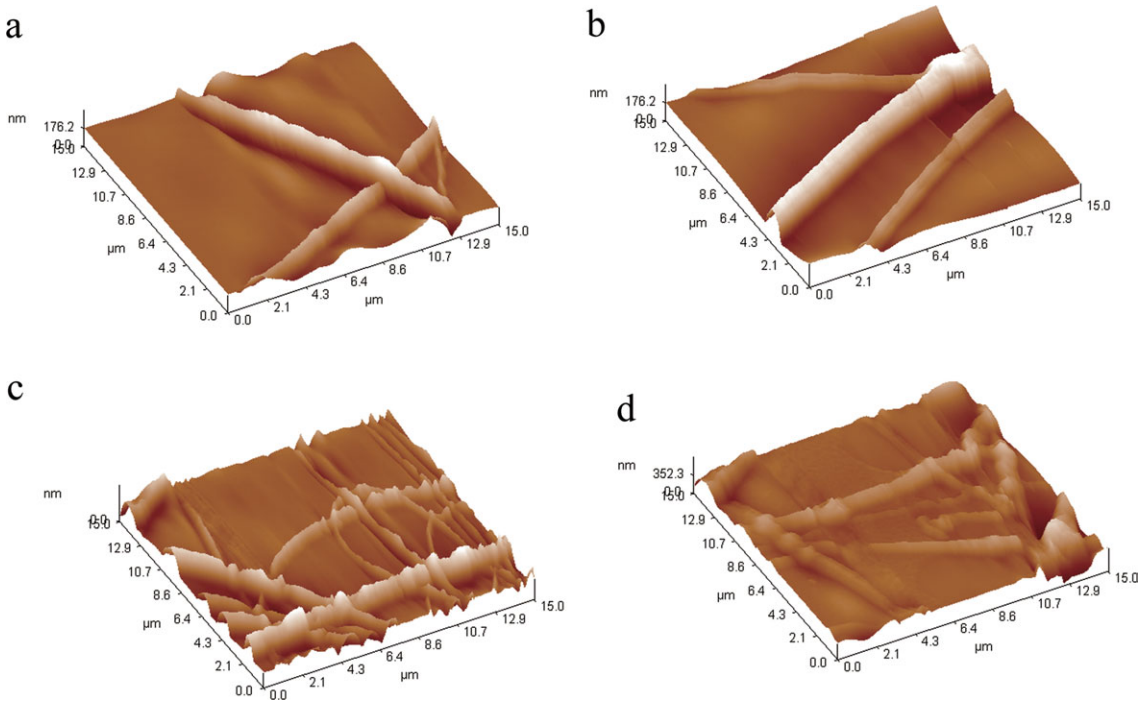

Figure 4. AFM images of the PAN and PAN/GO composite nanofibers: (a) PAN, (b) PAN/GO-0.05, (c) PAN/GO-0.1, and (d) PAN/GO-0.5. [Color figure can be viewed in the online issue, which is available at wileyonlinelibrary.com.]

The dispersion of GO in PAN composite nanofibers was characterized by HRTEM. The HRTEM images of pure PAN and PAN/GO-0.1 composite nanofibers are presented in Figure 5(a,b). The transmission electron microscopy (TEM) image clearly revealed that the clusters of GO nanoplatelets were well incorporated in the polymer matrix and oriented in the fiber axial direction, which was due to the higher draw ratio that imparted a larger stress on the fiber as it was being formed during the electrospinning process and gave rise to a proper alignment of the two-dimensional GO pallets along the fiber axis. Besides, with GO as nanofiller, the surface of the composite nanofibers became rough and irregular, which was in accordance with the results of AFM observations.

The lateral contrast properties can be seen in Figure 5. The darker regions represent low lateral forces and lighter ones the opposite. It can be observed that with the addition of GO, the friction properties of the specimen surface greatly changed. For pure PAN [Figure 5(c)], the surface was quite uniform in friction properties due to the fact that the fiber was made up of single phase. When the concentration of GO was 0.1 wt % [Figure 5(b)], a lighter line parallel to the fiber's axis was observed on the surface of the composite nanofiber, which confirmed the TEM observations. So the inhomogeneous dispersion of GO inside the polymer matrix contributed to the different surface friction properties of the fiber. The GO-rich region had a higher lateral force.

Nanomechanical Properties

The force induced by the tip during the process that the cantilever approached and retracted from the surface of the sample was recorded by the force–distance curve; this provided abundant information about the elastic properties of the sample's surface. Figure 4(a) presents a representative force–distance curve recorded on the pure superficial PAN nanofibers, and Figure 4(b) shows the retraction curves obtained when different concentrations of GO were added and the corresponding deflective values calculated from the curves.

The curve starts at point A, where there was no obvious deflection of the cantilever. Interestingly, the flat baseline did not coincide with the zero-force level was measured at infinite separation but was lower; this was attributed to an ultra-long-range attractive force acting at a distance and, thus, well beyond the maximum z range for recording in force curves.[17] As the piezo moved toward the sample, the tip jumped into contact with the adsorbed water film and wicked up around it to form a meniscus. This contributed to the sudden mechanical instability occurred between points B and C. The cantilever bent downward because of the attractive meniscus force acting on the tip. As the piezo further approached the sample surface, the deflection of the cantilever increased when the tip traveled in the water film. Eventually, it contacted the underlying nanofiber surface and carved into the nanofiber when it started to bend upward.[18] Once the cantilever reached the designated value of induced force at point D (D′), it retracted to its starting position. Because of the adhesion or chemical-bond formed during the process of contact, the tip went beyond zero deflection (point E). When the cantilever continued to move away from the sample, the elastic force of the cantilever became equivalent to the adhesive force and caused the cantilever snap back to point F. The cantilever reached its normal state with no deflection again.

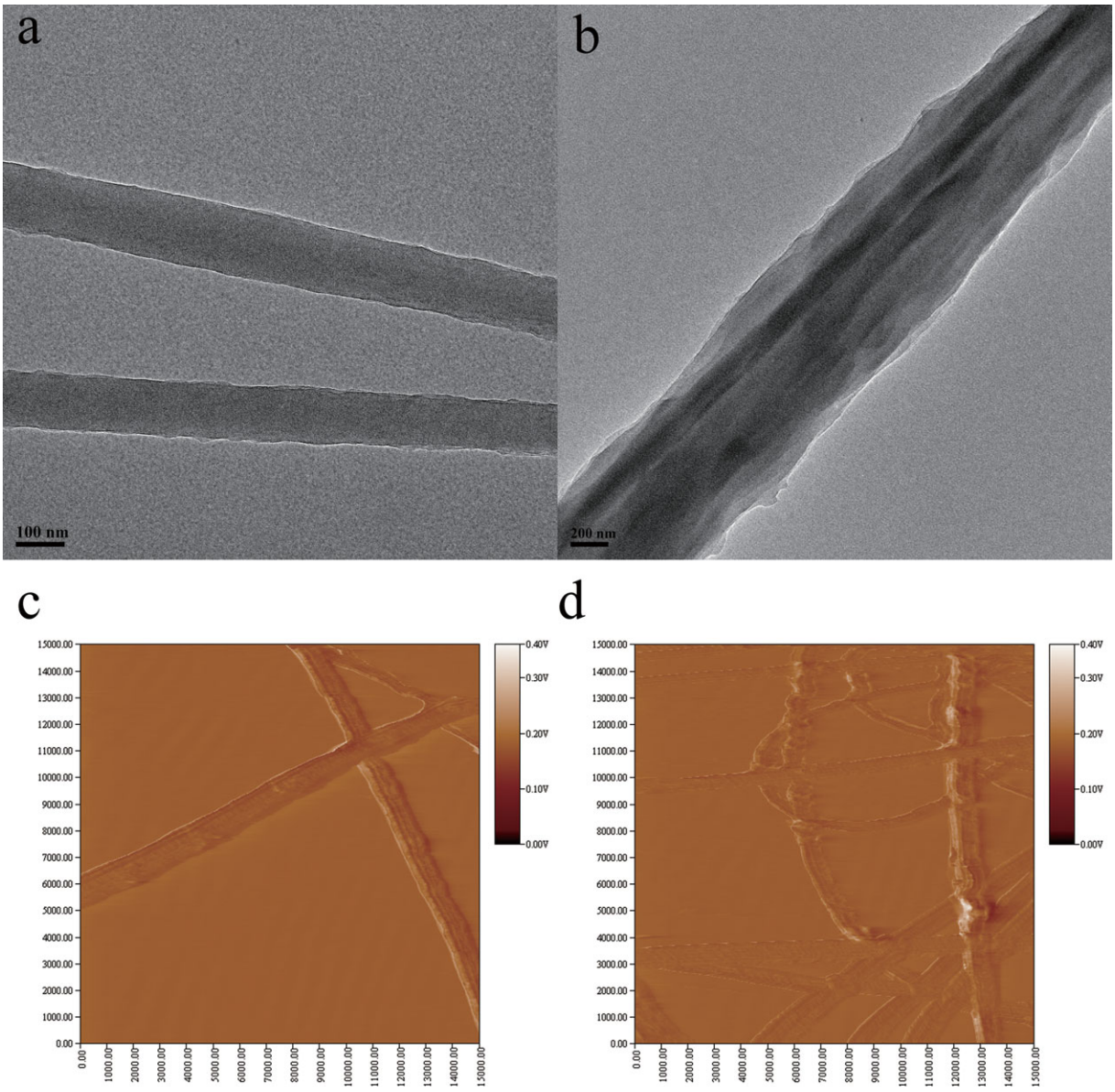

Figure 5. LFM and TEM images of the PAN and PAN/GO composite nanofibers: (a) LFM image of PAN, (b) LFM image of PAN/GO-0.1, (c) TEM of PAN, and (d) TEM of PAN/GO-0.1. [Color figure can be viewed in the online issue, which is available at wileyonlinelibrary.com.]

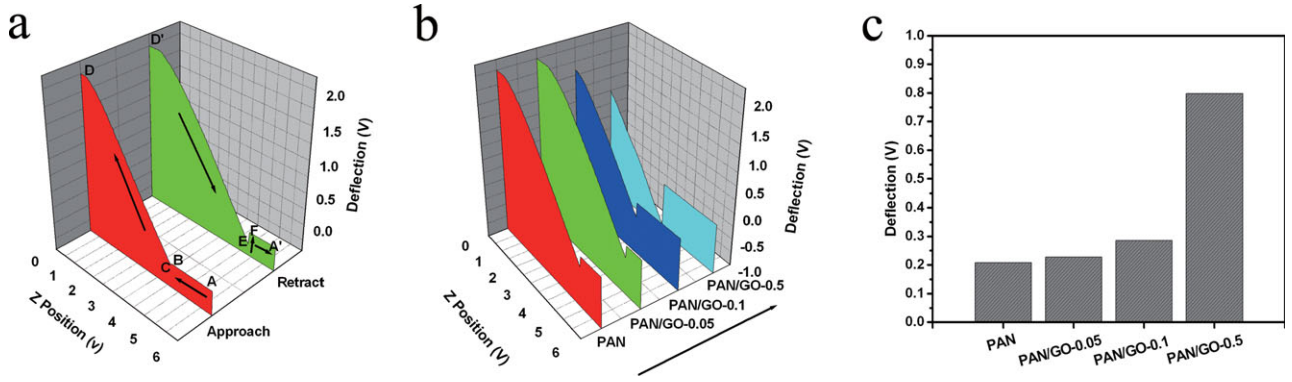

Figure 6. Surface nanomechanical properties of PAN/GO composite nanofibers. (a) An example of a force–distance curve for the investigated pure PAN sample, (b) the retract data of the force–distance curve obtained when different amounts of GO were added, and (c) the deflection data calculated from the data in part b. [Color figure can be viewed in the online issue, which is available at wileyonlinelibrary.com.]

The adhesive force between the tip and sample was calculated from the force–distance curve by multiplication of the vertical distance between E and F with the stiffness of the cantilever;[18] this meant that the adhesive force was proportional to the vertical distance, as the cantilever stiffness was a constant. From Figure 4(b), it can be seen that the addition of different amounts of GO contributed to the increase of the adhesive force to various extents, especially for the sample with 0.5 wt % GO; the induced force was almost four times the one without GO addition. The oxygen atoms in GO formed hydrogen-bonding interactions with the then PAN chains, which was proven by FTIR analysis. The intermolecular hydrogen-bonding interactions increased the elasticity of the polymer host.[19,20] Also, under ambient conditions, another dominant force was capillary force because of the formation of a liquid meniscus between the tip and the surface.[21] With the addition of GO, the quantity of surface-bound water increased. So, when the concentration of GO was 0.5 wt %, the surface water film bound by oxygen containing groups of GO contributed to the increased adhesive force.

CONCLUSIONS

PAN and PAN/GO composite nanofibers were prepared, and their surface properties were analyzed and compared. The effects of GO addition on the fibrous structure, chemical properties, surface morphology, friction, and elastic properties were investigated. The results reveal that with the increase of GO addition, the average diameter of the nanofibers decreased, and beaded structures were formed. Also, the use of GO as a nanofiller also increased the surface roughness, the friction force, and the elasticity.

ACKNOWLEDGMENTS

This work was supported financially by the National High-Tech. R&D Program of China (Contract grant number: 2012AA030313), Changjiang Scholars and Innovative Research Team in University (contract grant number IRT1135), National Natural Science Foundation of China (contract grant numbers 51006046 and 51163014), the Priority Academic Program Development of Jiangsu Higher Education Institutions, Specialized Research Fund for the Innovation Project of Jiangsu Graduate Education (contract grant number CXZZ11_0471), and the Research Fund for Doctoral Program of Higher Education of China (contract grant number 20090093110004).

REFERENCES

1. Rahaman, M. S. A.; Ismail, A. F.; Mustafa, A. *Polym. Degrad. Stab.* **2007,** *92*, 1421.
2. Qiao, H.; Cai, Y.; Chen, F.; Wei, Q. *Fibers Polym.* **2009,** *10*, 750.
3. Zhang, L.; Hsieh, Y.-L. *Eur. Polym. J.* **2009,** *45*, 47.
4. Chakrabarti, K.; Nambissan, P. M. G.; Mukherjee, C. D.; Bardhan, K. K.; Kim, C.; Yang, K. S. *Carbon* **2006,** *44*, 948.
5. Cassagneau, T.; Guerin, F.; Fendler, J. H. *Langmuir* **2000,** *16*, 7318.
6. Pumera, M. *Chem. Soc. Rev.* **2010,** *39*, 4146.
7. Kovtyukhova, N. I.; Ollivier, P. J.; Martin, B. J.; Mallouk, T. E.; Chizhik, S. A.; Buzaneva, E. V.; Gorchinskiy, A. D. *Chem. Mater.* **1999,** *11*, 771.
8. Li, D.; Xia, Y. N. *Adv. Mater.* **2004,** *16*, 1151.
9. Greiner, A.; Wendorff, J. H. *Angew. Chen. Int. Ed.* **2007,** *46*, 5670.
10. Shui, J. L.; Li, J. C. M. *Nano Lett.* **2009,** *9*, 1307
11. Bao, Q.; Zhang, H.; Yang, J.-X.; Wang, S.; Tang, D. Y.; Jose, R.; Ramakrishna, S.; Lim, C. T.; Loh, K. P. *Adv. Funct. Mater.* **2010,** *20*, 782.
12. Stankovich, S.; Dikin, D. A.; Dommett, G. H. B.; Kohlhaas, K. M.; Zimney, E. J.; Stach, E. A.; Piner, R. D.; Nguyen, S. T.; Ruoff, R. S. *Nature* **2006,** *442*, 282.
13. Saeed, K.; Haider, S.; Oh, T. J.; Park, S. Y. *J. Membr. Sci.* **2008,** *322*, 400.
14. Si, Y.; Samulski, E. T. *Nano Lett.* **2008,** *8*, 1679.
15. Stankovich, S.; Piner, R. D.; Nguyen, S. T.; Ruoff, R. S. *Carbon* **2006,** *44*, 3342.
16. Shao, D.; Wei, Q.; Zhang, L.; Cai, Y.; Jiang, S. *Appl. Surf. Sci.* **2008,** *254*, 6543.
17. Jones, R.; Pollock, H. M.; Geldart, D.; Verlinden, A. *Powder Technol* **2003,** *132*, 196.
18. Zaghloul, U.; Bhushan, B.; Papaioannou, G.; Coccetti, F.; Pons, P.; Plana, R. *J. Colloid Interface Sci.* **2012,** *365*, 236.
19. Roland, C. M.; Casalini, R. *Macromolecules* **2003,** *36*, 1361.
20. Shawn, J.; Karl, I. J.; Satish, K. *J. Polym. Sci. Part B: Polym. Phys.* **2000,** *38*, 3053.
21. Pelin, I. M.; Piednoir, A.; Machon, D.; Farge, P.; Pirat, C.; Ramos, S. M. M. *J. Colloid Interface Sci.*, to appear.